가속도계의 동작범위 확장와 선형성 향상을 위한 피드백 제어

Feedback Control for Expanding Range and Improving Linearity of Microaccelerometers

박 용 화, 박 상 준, 최 병 두, 고 형 호, 송 태 용, 임 근 원, 허 건 수, 박 장 현, 조 동 일*

(Yonghwa Park, Sangjun Park, Byungdoo Choi, Hyoungho Ko, Taeyong Song, Geunwon Lim,
Kunsoo Huh, Jahng-hyon Park, and Dong-il "Dan" Cho)

Abstract : This paper presents a feedback-controlled, MEMS-fabricated microaccelerometer (µXL). The µXL has received much commercial attraction, but its performance is generally limited. To improve the open-loop performance, a feedback controller is designed and experimentally evaluated. The feedback controller is applied to the x/y-axis µXL fabricated by sacrificial bulk micromachining (SBM) process. Even though the resolution of the closed-loop system is slightly worse than open-loop system, the bandwidth, linearity, and bias stability are significantly improved. The noise equivalent resolution of open-loop system is 0.615 mg and that of closed-loop system is 0.864 mg. The bandwidths of open-loop and closed-loop system are over 100 Hz. The input range, non-linearity and bias stability are improved from ±10 g to ±18 g, from 11.1 %FSO to 0.86 %FSO, and from 0.221 mg to 0.128 mg by feedback control, respectively.

Keywords : microaccelerometer, feedback control, modeling, simulation

I. Introduction

Micro-fabricated accelerometers have received much commercial attraction due to the small size, low power consumption, rigidity, and low cost[1]. However, because of the very small size, the open-loop performance is generally limited. To improve the open-loop performance, we design a feedback controller in this paper. The closed-loop system feeds the control signal from the sensed output signal back to the feedback control electrodes. This makes the displacement of the moving parts very small, and the bandwidth of the system is increased. Furthermore, because the displacement of the moving parts is controlled to be small, the linearity of the output signal can be improved.

II. Working principle

Figure 1 shows the x/y-axis µXL with feedback control electrodes. A quarter of sensing electrodes are used as feedback control electrode. The SBM-fabricated µXL has a 40 µm of structural thickness and a 20 µm of sacrificial gap. The SBM process has the added benefits of a large sacrificial gap when compared to conventional SOI process[2-4].

Figure 2 shows the schematics of µXL and readout circuit. The inertia force exerted by applied acceleration compels the proof mass to move, and this motion produces the capacitance change. The capacitance change is detected by a charge-to-

voltage converter. After the high-pass filtering, the signal is demodulated using an analog multiplier. After low-pass filtering, the demodulated acceleration signal is obtained without the high frequency components.
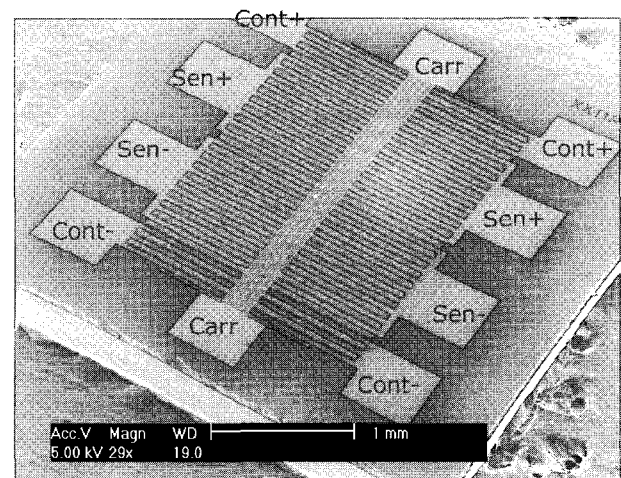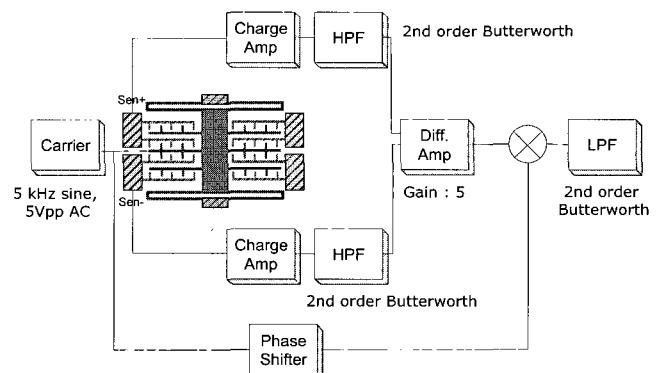

Fig. 1. Fabricated microaccelerometer.

Fig. 2. Schematics of µXL and readout circuit.

III. Dynamic modeling

The μXL consists of proof mass, flexures, sensing combs, and control combs as shown in Figure 1. The dynamics of the μXL can be simply modeled as a mass-damper-spring system as showed in Figure 3. The equation of the sensing motion is given by

$$m\ddot{x} + b\dot{x} + kx = ma \tag{1}$$

where m, b, k are mass, damping, and spring coefficient of the sensing mode, respectively; x is displacement of the proof mass and a is an external acceleration.
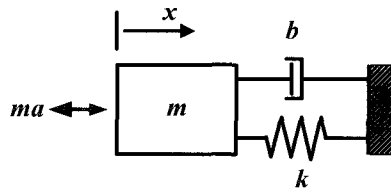

Fig. 3. Modeling of the μXL.

The μXL has a structural thickness of 40 μm, a lateral gap between electrodes of 1.5 μm, and a spring length of 452 μm. The values of m, b, and k can be obtained from the structure of the μXL and the equations of relation between the resonant frequency, quality factor, and damping coefficient. The resonant frequency and quality factor are given by

$$f = \frac{1}{2\pi}\sqrt{\frac{k}{m}} \tag{2}$$

$$\frac{1}{Q} = \frac{\mu A \beta}{\sqrt{mk}\left(\dfrac{\cosh 2\beta d - \cos 2\beta d}{\sinh 2\beta d + \sin 2\beta d}\right)} + \frac{\mu A_c \beta}{\sqrt{mk}\left(\dfrac{\cosh 2\beta d_c - \cos 2\beta d_c}{\sinh 2\beta d_c + \sin 2\beta d_c}\right)} + \frac{\mu t W^3}{d_2^{\,3}\sqrt{mk}} \tag{3}$$

where μ, β, A, A_c, d, d_c, d_2, t, and W are absolute viscosity, momentum propagation velocity, area of plate, areas of inter-comb, sacrificial gap, lateral gap between combs, gap between structure and comb, structural thickness, and width of comb, respectively[5-6]. Also, damping coefficient is given by

$$b = \frac{\sqrt{mk}}{Q}. \tag{4}$$

The calculated mass, m, is 122 μg. By ANSYS simulation, the first mode resonant frequency is 1 kHz. From Eq. (2), the value of k is 4.82 N/m. From Eqs. (3) - (4), the value of b is 1.917×10^{-5} kg/s.

IV. Controller Design

Figure 4 shows the block diagram of the closed-loop system. The plant G(s) consists of the sensing dynamics of the μXL, the charge amplifier, the high-pass filter, and the differential

amplifier, which are shown in Figure 2. This plant G(s) can be modeled as a simple 2nd-order transfer function as follows;

$$G(s) = \frac{4.86 \times 10^{12}}{s^2 + 157s + 3.95 \times 10^7}. \tag{5}$$

The damping ratio of this plant is very small. So, the overshoot of this plant is very large and the settling time is very long. Figure 5 shows the step response of the open-loop system. The settling time is 49.5 ms and the modulated output signal is 15 mV.

If an external acceleration is applied to the accelerometer, the proof mass should quickly reach the position as much as the magnitude of acceleration. Then the accelerometer should be ready to receive some other external acceleration. So, the feedback controller K(s) is designed to reduce the settling time of this system and increase the damping ratio. A simple controller that satisfies this condition is a PD controller. The feedback controller K(s) is given by

$$K(s) = K_P(1 + T_D s) \tag{6}$$

where K_P is the proportional feedback gain, and T_D is the derivative rate.

First of all, the suitable value of T_D is selected. When the value of T_D is 0.001 sec, the value of K_P can be easily selected using the root locus technique. If the value of K_P is 4.2, the damping ratio is 0.718 and the step response of the closed-loop system is obtained as shown in Figure 6. The settling
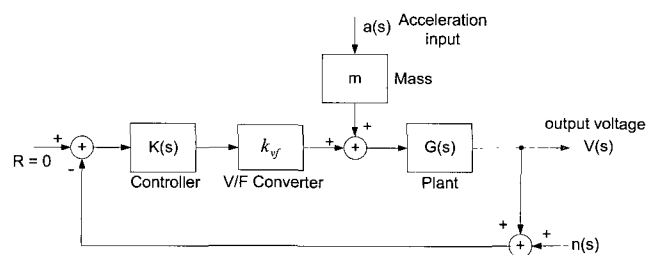

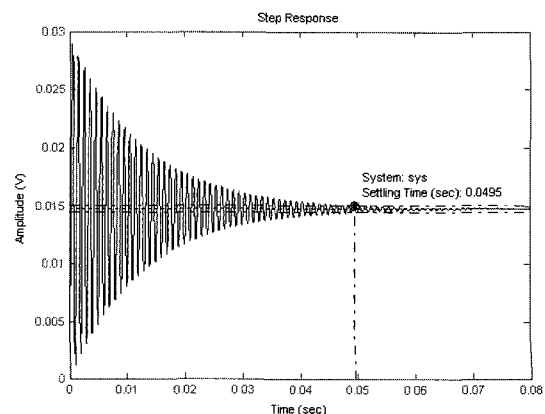Fig. 4. Block diagram of the closed-loop system.

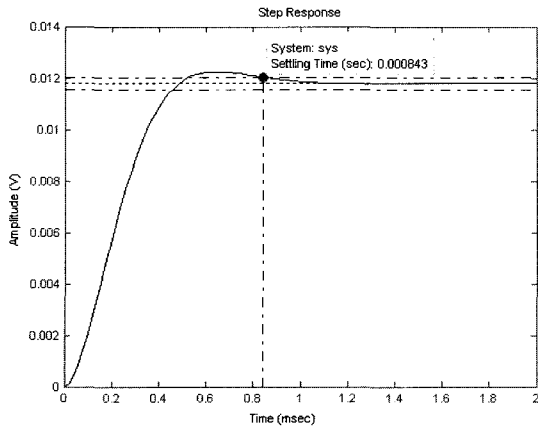Fig. 5. Step response of the open-loop system.

Fig. 6. Step response of the closed-loop system.

time of the closed-loop system is reduced from 49.5 ms to 0.843 ms, and the modulated output signal is decreased from 15 mV to 12 mV, when compared to the open-loop system.

V. Simulation results

We use the MATLAB SIMULINK as the simulation program. Figure 7 shows the SIMULINK block diagram of the closed-loop system. With the input acceleration of 1 g at 40 Hz, Figure 8 shows the frequency response of the modulated output signal. Because the average output signal is decreased, the noise equivalent input acceleration resolution of the closed-loop system gets worse from 0.192 mg to 0.237 mg, when compared to the open-loop system. But the noise floor of the closed-loop system is also decreased. The average output signal level and the noise floor of the open-loop system are -17.2 dB and -91.5 dB, respectively, and the average output signal level and the noise floor of closed-loop system
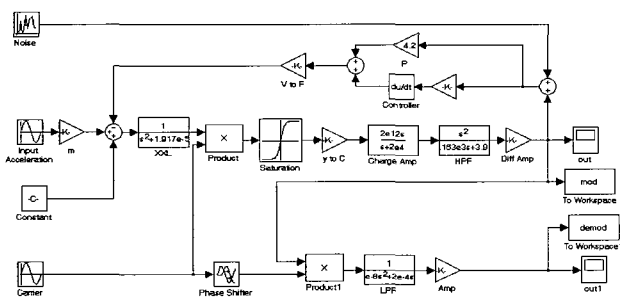
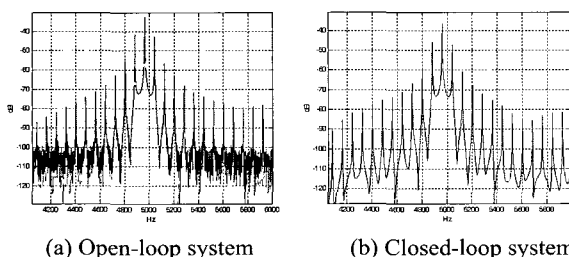

Fig. 7. SIMULINK block diagram of the closed-loop system.

(a) Open-loop system   (b) Closed-loop system

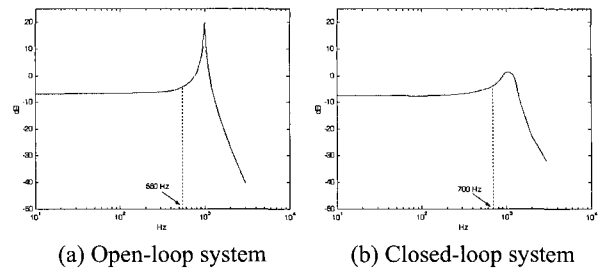Fig. 8. Frequency response of the modulated output signal at 40 Hz, 1g input acceleration.

(a) Open-loop system   (b) Closed-loop system

Fig. 9. Bode diagram of the demodulated output signal.

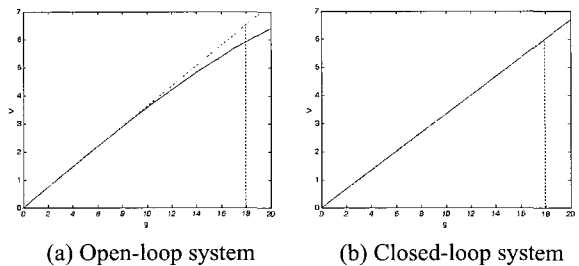(a) Open-loop system   (b) Closed-loop system

Fig. 10. Linearity and input range of the output signal.

are -21.3 dB and -93.8 dB, respectively.

Figure 9 shows the bode diagram of the demodulated output signal. This output signal is obtained by increasing the period of input acceleration. The bandwidth of the closed-loop system is improved from 550 Hz to 700 Hz. Figure 10 shows the demodulated output signal when the magnitude of input acceleration varies. The scale factor of the closed-loop system is decreased to 0.41 V/g from 0.35 V/g of the open-loop system. The input range of the closed-loop system is improved from ±10 g to ±18 g. Also, the non-linearity of the closed-loop system is improved from 11 %FSO to 0 %FSO in the ±18 g range.

VI. Experimental results

Figure 11 shows the closed-loop implementation of μXL. After a 5 volt peak-to-peak sinusoidal voltage without offset voltage is applied to the proof mass of the μXL, we measure the output voltage when an external acceleration is applied using the shaker table as shown in Figure 12.
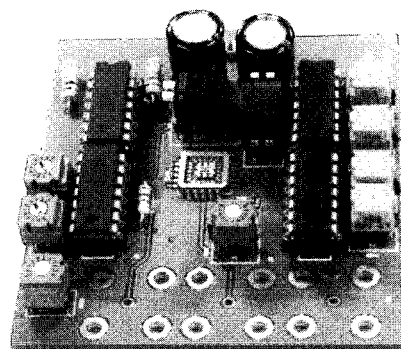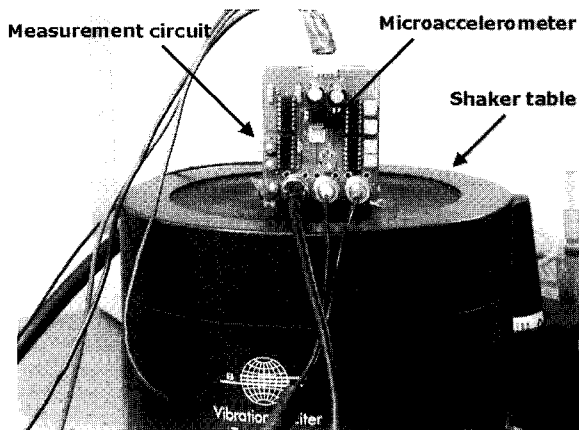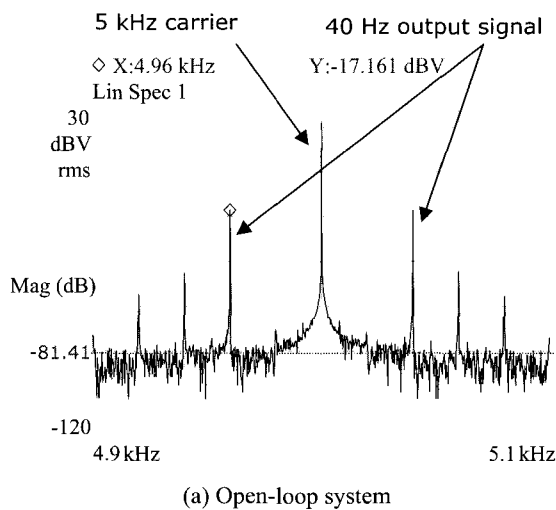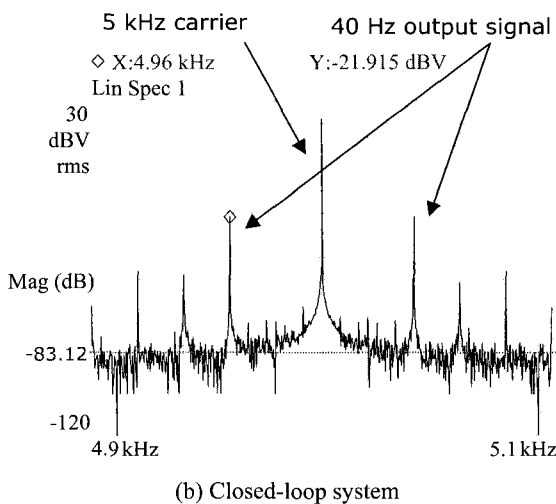

Fig. 11. Closed-loop implementation of μXL.

Fig. 12. Experimental setup using the shaker table.

5 kHz carrier   40 Hz output signal

◇ X:4.96 kHz   Y:-17.161 dBV
Lin Spec 1
30
dBV
rms

Mag (dB)

-81.41

-120
4.9 kHz   5.1 kHz

(a) Open-loop system

5 kHz carrier   40 Hz output signal

◇ X:4.96 kHz   Y:-21.915 dBV
Lin Spec 1
30
dBV
rms

Mag (dB)

-83.12

-120
4.9 kHz   5.1 kHz

(b) Closed-loop system

Fig. 13. Frequency response of the modulated output signal at
40 Hz, 1g input acceleration.

Figure 13 shows the modulated output signal of the
fabricated accelerometer when the input acceleration of 1 g at
40 Hz is applied. The noise equivalent input acceleration
resolution, the average output signal level, and the noise floor
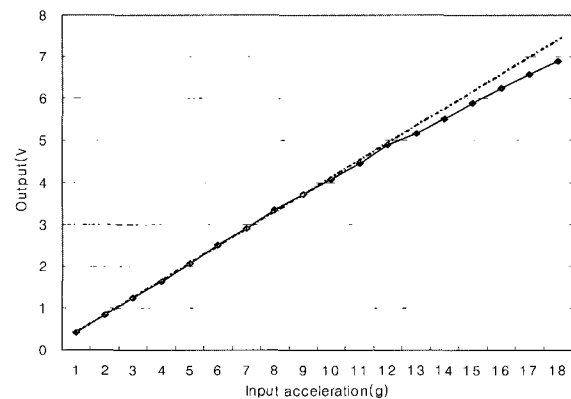of the closed-loop system are all decreased such as the
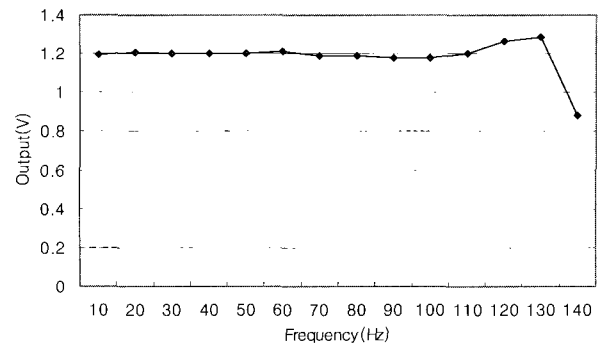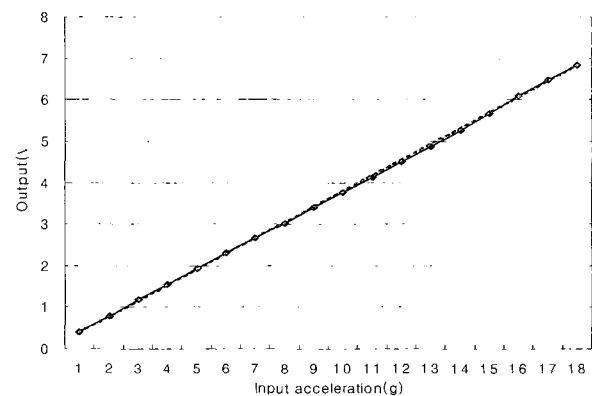

(a) Open-loop system
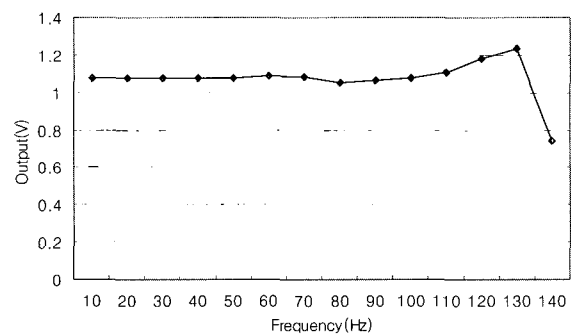
(b) Closed-loop system

Fig. 14. Frequency response of the demodulated output signal.

(a) Open-loop system

(b) Closed-loop system

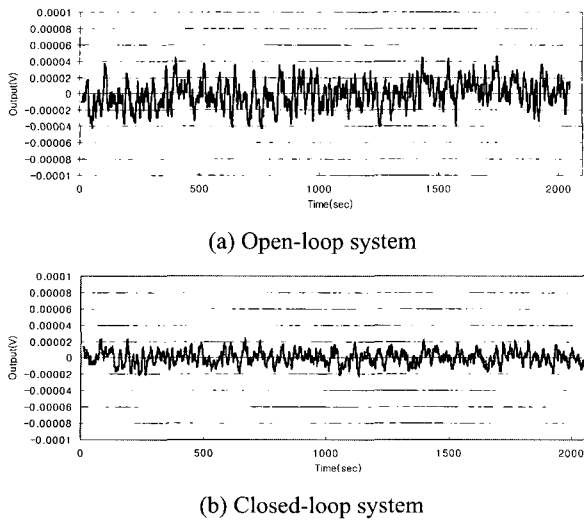Fig. 15. Linearity and input range at 40 Hz.

(a) Open-loop system

(b) Closed-loop system

Fig. 16. Bias stability of the demodulated output signal.

Table 1. Performance summary of the system.

	Open-loop system	Closed-loop system
Resolution	0.615 mg	0.864 mg
Noise floor	-81.41 dB	-83.12 dB
Bandwidth	–	–
Input range	±10 g	±18 g
Non-linearity (in 18 g range)	11.12 %FSO	0.86 %FSO
Bias stability	0.221 mg	0.128 mg

simulation result, when compared to the open-loop system. The noise equivalent input acceleration resolution of the closed-loop system gets worse from 0.615 mg to 0.864 mg. The average output signal level and the noise floor of the open-loop system are -17.19 dB and -81.41 dB, respectively, and the average output signal level and the noise floor of closed-loop system are -21.85 dB and -83.12 dB, respectively. Because the noise floor of the measurement result is larger than the simulation result, the resolution of the measurement result becomes worse than the simulation result. The measurement circuit and the measurement environment should be improved to solve this noise problem.

Figure 14 shows the frequency response of the demodulation output signal. The frequency response of the open-loop and closed-loop system are measured only up to the shaker table limit of 100 Hz. The bandwidth cannot be measured using the shaker table. Figure 15 shows the linearity of the output signal when the magnitude of input acceleration varies at 40 Hz. We obtain the similar result with the simulation result. The scale factor of the closed-loop system is decreased to 0.376 V/g from 0.406 V/g of the open-loop

system. The input range of the closed-loop system is improved from ±10 g to ±18 g. Also the non-linearity of the closed-loop system is improved from 11.12 %FSO to 0.86 %FSO in the ±18 g range. Finally, the bias stability tests are performed. Figure 16 shows the demodulated output signal without applied the input acceleration. The bias stability of the closed-loop system is improved from 0.221 mg to 0.128 mg. The specifications are summarized in table 1.

VII. Conclusions

In this paper, a simple PD controller is designed for a MEMS μXL. Using this simple controller, the performances of the μXL such as the bandwidth, linearity, and bias stability are improved by feeding the control signal from the sensed output signal back to the sensing-comb electrodes. The most dramatic improvements are in the range and linearity. The input range is improved from ±10 g to ±18 g, and the non-linearity is improved from 11.12 % FSO to 0.86 %FSO. The resolution is slightly degraded from 0.615 mg to 0.864 mg, which is attributed to the additional electrodes. However, the more important measure relating to resolution is bias stability, and the bias stability is improved from 0.221 mg to 0.128 mg. This bias stability improvement is achieved because the closed-loop system can maintain the proof mass at the zero position better than the open-loop system in the absence of external accelerations.

REFERENCES

[1] C. Song, "Commercial vision of silicon based inertial sensors", Proceeding of Transducer '97, vol. 2, pp. 839-842, 1997.

[2] S. Lee, S. Park, and D. Cho, "The surface/bulk micromachining(SBM) process: a new method for fabricating released microelectromechanical systems in single crystal silicon", IEEE/ASME Journal of Microelectromechanical Systems, vol. 8, no. 4, pp. 409-416, 1999.

[3] S. Lee, S. Park, J. Kim, S. Yi, and D. Cho, "Surface/bulk micromachined single-crystalline silicon micro-gyro-scope", IEEE/ASME Journal of Microelectromechanical Systems, vol. 9, no. 4, pp. 557-567, 2000.

[4] D. Cho, S. Lee, and S. Park, "Surface/bulk micromachined high performance silicon micro-gyroscope" 2000 Solid-state Sensor and Actuator Workshop (Hilton Head), 2000.

[5] Y. H. Cho, B. M. Kwak, A. P. Pisano, and R. T. Howe, "Viscous energy dissipation in laterally oscillating planar microstructures: A theoretical and experimental study" Proc. IEEE Workshop on Microelectro-mech. Sys., pp. 93-99, 1993

[6] B. R. Munson "Fundamentals of Fluid Mechanics", 2nd edition.

Yonghwa Park

He received the B.S. degree in electrical engineering from KAIST, Daejeon, Korea, in 2000. He is currently a M.S. candidate in electrical engineering and computer science from Seoul National University. His research interests include the design and control of MEMS inertia sensor.

Sangjun Park

He received the B.S., M.S., and Ph.D degrees in electrical engineering and computer science from Seoul National University, Seoul, Korea, in 1997, 1999 and 2004, respectively, where he is currently postdoctoral researcher in the School of Electrical Engineering and Computer Science. His research interests include design, optimization, and fabrication of microactuators and microinertial sensors.

Byungdoo Choi

He received the B.S. degrees in electrical engineering from KAIST, Dajeon, Korea, in 2001, where he is currently working toward the Ph.D. degree in the School of Electrical Engineering and Computer Science from Seoul National University, Seoul, Korea. His research interests include design, optimization, and fabrication of microactuators and microinertial sensors.
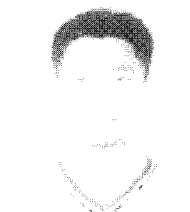
Hyoungho Ko

He received the B.S. degrees in electrical engineering and computer science from Seoul National University, Seoul, Korea, in 2002, where he is currently working toward the Ph.D. degree in the School of Electrical Engineering and Computer Science. His research interests include interface circuit design, Si fabrication and testing of microinertial sensors.

Taeyong Song

He received the B.S degrees in electrical and electronic engineering from Yonsei University, Seoul, Korea, in 2002, where he is currently working toward the M.S degree in electrical engineering and computer science from Seoul National University, Seoul, Korea. His research interests include mechanical analysis, simulation of microstructures, Si fabrication and testing of microinertial sensors.

Geunwon Lim

He received the B.S. degree in electrical engineering and computer science from University of Seoul, Seoul, Korea, in 2000. He is currently working in the School of Electrical Engineering and Computer Science. His research interests include optimization, Si fabrication and package for microinertial sensors.

Kunsoo Huh

He received the B.S. degree in mechanical engineering from the Seoul National University, Korea, in 1982, the M.S. degree in mechanical engineering from the KAIST, Korea, in 1984, and the Ph.D. degree in mechanical engineering from the University of Michigan, Ann Arbor, USA, in 1992. In 1993, he joined the School of Mechanical Engineering at the Hanyang University, Seoul, Korea, where he is currently a Associate Professor. His research interests include machine monitoring and control, with application to intelligent vehicles, tracked vehicles, machine tools and nano/micro stages.
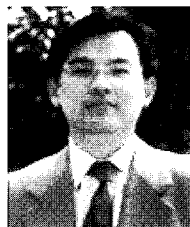
Jahng-hyon Park

He received the B.S. and M.S. degrees from Seoul National University, Seoul, Korea, in 1983 and 1985 and the Ph. D. degree from Massachusetts Institute of Technology, Cambridge, in 1992, respectively, where he is currently professor in the School of Mechanical Engineering, Hanyang University. His research interests include intelligent machine.
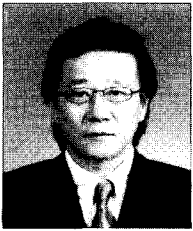
Dong-il "Dan" Cho

He received the BSME degree from Carnegie-Mellon University, Pittsburgh, PA, in 1980 and the SM and Ph.D. degrees from Massachusetts Institute of Technology, Cambridge, in 1984 and 1987, respectively. From 1987 to 1993, he was assistant professor in the Mechanical and Aerospace Engineering Department, Princeton University, Princeton, NJ. In 1993, he joined the Department of Control and Instrumentation Engineering, Seoul National University, Seoul, South Korea, where he is currently professor in the School of Electrical Engineering and Computer Science. He is the director of Microsystem Technology Center since 2002. He is also the chairman of Korea MEMS association since 2003. His research interests include silicon micro and nano processes, silicon micro accelerometers and gyroscopes, silicon nano tips, bio electronics, and RF MEMS.